Scientia Iranica, Vol. 11, Nos. 1&2, pp 114–120

SCIENTIA IRANICA

Research Note

Flow over Triangular Side Weir

M. Ghodsian[1]

In this paper, the hydraulic characteristics of a sharp crested triangular side weir have been experimentally studied. It was found that the DeMarchi coefficient of discharge for a sharp crested triangular side weir in subcritical flow is related to the main channel Froude number, the apex angle of weir and ratio of weir height to upstream depth of flow. Suitable equations for discharge coefficient are also obtained.

INTRODUCTION

A side weir is an overflow and metering diversion structure set into the side of a channel with the purpose of allowing part of the liquid to spill over the side, if the surface of the flow in the channel rise above the weir crest. Side weirs are typically used in irrigation, land drainage, urban sewage systems and sanitary engineering and are also widely used for storm relief, as well as head regulators of distributaries.

The flow over a side weir is a typical case of spatially varied flow with decreasing discharge. The discharge over the side weir is affected by the main channel velocity. Like normal weirs, side weirs may be of different shapes (i.e., rectangular, triangular, trapezoidal etc.). Further, side weirs may be made sharp or broad crested. Sharp crested rectangular side weirs have been studied extensively by many investigators [1-15]. It is obvious that almost all the investigators have studied the hydraulic characteristics of rectangular side weirs and less attention has been given to the behavior of flow over triangular side weirs. Kumar and Pathak [16] related the discharge coefficient of a triangular side weir to approach Froude number and apex angle of the weir.

In this paper, experimental results on sharp crested triangular side weirs with apex angles of 30, 60, 90 and 120 degrees, respectively, are reported. New equations for the discharge coefficient are introduced. It was found that the discharge coefficient, in addition to approach Froude number, is a function of apex angle and ratio of weir height to upstream depth of flow. The experiments were restricted to subcritical flow in the main channel and free flow in the side channel.

1. *Department of Civil Engineering, Tarbiat Modarres University, Tehran, I.R. Iran.*

BASIC THEORY

The flow over a side weir is a typical case of spatially varied flow with decreasing discharge. The energy equation is commonly used for deriving the governing equation for the flow over a side weir. The general differential equation of spatially varied flow along a side weir (Figure 1) with decreasing discharge, was given by Henderson as [17]:

$$\frac{dy}{dx} = \frac{S_0 - S_f - \alpha \frac{Q dQ}{g A^2 dx}}{1 - \alpha \frac{Q^2 T}{g A^3}}, \qquad (1)$$

in which y = depth of flow, x = distance along side weir from upstream end, S_0 = main channel slope, S_f =

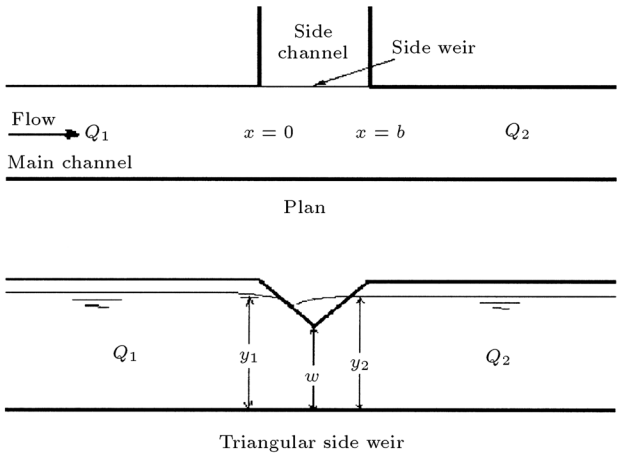

Figure 1. Subcritical flow over triangular side weir.

friction slope, α = kinetic energy correction factor, Q = discharge in channel, dQ/dx = discharge per unit length of side weir, g = acceleration due to gravity, A = cross-sectional area of flow and T = top width of the channel section.

For a horizontal ($S_0 = 0$) prismatic rectangular main channel, assuming the kinetic energy correction factor α as unity and neglecting friction losses ($S_f = 0$), Equation 1 is simplified as:

$$\frac{dy}{dx} = \frac{Q\,y}{gB^2y^3 - Q^2}\left(-\frac{dQ}{dx}\right), \tag{2}$$

in which B is the width of main channel.

The discharge per unit length of a triangular side weir is calculated by the following equation, as presented by Kumar and Pathak [16]:

$$\frac{dQ}{dx} = -\frac{4}{15}C_m\sqrt{2g}(y-w)^{1.5}, \tag{3}$$

in which C_m is the side weir discharge coefficient, known as the DeMarchi coefficient of discharge and w is the side weir apex height.

By assuming that the specific energy, E, is constant along the length of the side weir, the discharge in the main channel, Q, is given by:

$$Q = By\sqrt{2g(E-y)}. \tag{4}$$

Combining Equations 2 to 4, one obtains:

$$\frac{dy}{dx} = \frac{8C_m}{15B}\frac{\left[(E-y)(y-w)^3\right]^{0.5}}{3y-2E}. \tag{5}$$

Integrating between the limits $x = 0$ and $x = b_1$ (i.e., sections 1 and 2 in Figure 1) and designating the two sections by suffixes 1 and 2, respectively, one gets:

$$b_1 = x_2 - x_1 = \frac{15B}{4C_m}(\phi_2 - \phi_1), \tag{6}$$

in which b_1 is the distance between sections 1 and 2 along the side weir and ϕ is the DeMarchi varied flow function, first derived by DeMarchi [17] as:

$$\phi = \frac{2E-3w}{E-w}\left(\frac{E-y}{y-w}\right)^{0.5} - 3\sin^{-1}\left(\frac{E-y}{E-w}\right)^{0.5}. \tag{7}$$

Equations 6 and 7 can be combined in the form of:

$$\frac{4b_1C_m}{15B} = \frac{2E-3w}{E-w}\left[\left(\frac{E-y_2}{y_2-w}\right)^{0.5} - \left(\frac{E-y_1}{y_1-w}\right)^{0.5}\right] - 3\left[\sin^{-1}\left(\frac{E-y_2}{E-w}\right)^{0.5} - \sin^{-1}\left(\frac{E-y_1}{E-w}\right)^{0.5}\right], \tag{8}$$

in which y_1 and y_2 are the depth of flow for sections 1 and 2, respectively (Figure 1). Equations 4 and 8 can be used to determine the discharge over the side weir. Knowing the upstream condition (Q_1 and E_1), channel and weir geometry (B, b_1, w and apex angle θ) and C_m, solve for y_2 using Equation 8, then find Q_2 using Equation 4. The discharge over the side weir, Q_s, is determined by:

$$Q_s = Q_1 - Q_2, \tag{9}$$

in which Q_1 and Q_2 are the discharges at sections 1 and 2 in the main channel, respectively. The values of C_m can be calculated from measured values of depth and discharge at sections 1 and 2, for a side weir with known geometry.

EXPERIMENTAL SETUP AND PROCEDURE

The experiments were conducted using a prismatic, horizontal channel. The main channel was 9.0 m long, 0.5 m wide and 0.5 m deep. The main and side channel were made of brick masonry and plastered with cement. A suitable sluice gate was provided at the downstream end of the main channel for maintaining the desired depth of flow in this channel. The side channel was constructed perpendicular to the main channel. The side weirs were made of mild steel plate, the top edge being suitably beveled to get a sharp crest. The side weir was installed at the upstream end of the side channel, flush with the main channel wall. Baffle walls were provided in the upstream of the channels, to get an inflow with little and acceptable disturbances.

Water was supplied to the main channel through a supply pipe, from an overhead tank at constant head and the flow was controlled by a gate valve. Calibrated sharp crested weirs were used for discharge measurement.

For a provided side weir, a certain discharge was allowed into the main channel and the desired depth of flow was obtained by the tailgate. Flow depths y_1 and y_2 (see Figure 1) were measured at the centerline of the main channel with a point gauge, having an accuracy of $\pm$ 0.1 mm. The discharges in the main channel extension and the side channel were also measured by calibrated sharp crested weirs. The experiments were repeated for various combinations of depth and discharge and for different apex angle and weir height. The range of various parameters covered in the present study is given in Table 1.

ANALYSIS OF DATA

Constancy of Energy

It was assumed by DeMarchi that the specific energy remains constant along the side weir. The present data

Table 1. Range of variables studied.

Apex Angle θ (°)	Side Weir Height w (m)	Upstream Depth y_1 (m)	Downstream Depth y_2 (m)	Upstream Discharge Q_1 (m^3/s)	Side Weir Discharge Q_s (m^3/s)
30	0–0.05	0.15–0.34	0.156–0.35	0.012–0.06	0.001–0.021
60	0–0.15	0.12–0.40	0.129–0.41	0.02–0.09	0.003–0.06
90	0–0.2	0.10–0.35	0.11–0.35	0.011–0.115	0.0007–0.046
120	0–0.15	0.07–0.26	0.08–0.27	0.005–0.086	0.0009–0.020

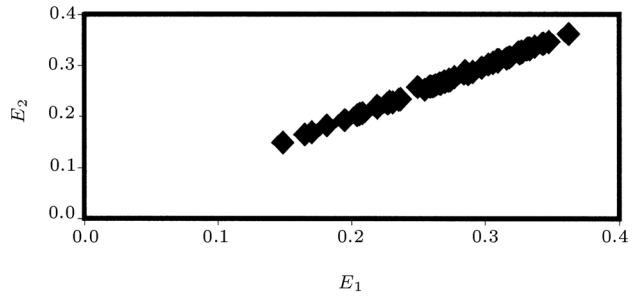

Figure 2. Comparison of specific energy E_1 and E_2 for apex angle = 30°.

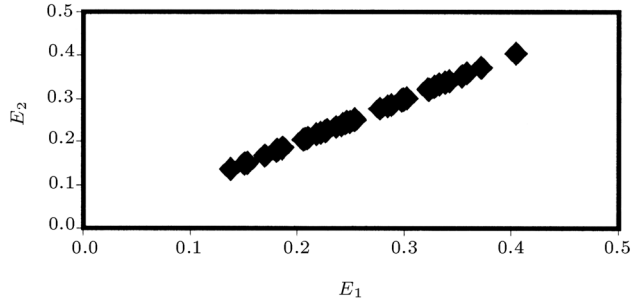

Figure 3. Comparison of specific energy E_1 and E_2 for apex angle = 60°.

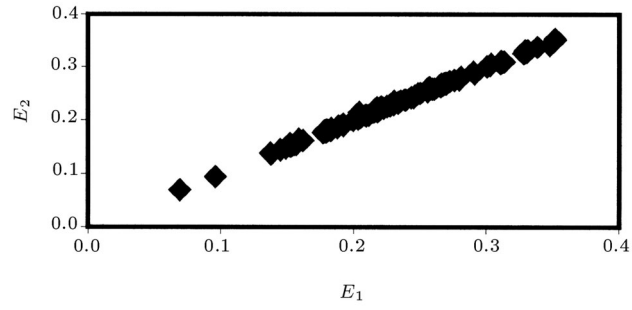

Figure 4. Comparison of specific energy E_1 and E_2 for apex angle = 90°.

were used in order to check this assumption. Figures 2 to 5 show the comparison of specific energy at the upstream, E_1, and downstream, E_2, of the side weir for different apex angles. The average energy difference between the two ends of a weir, for apex angles of

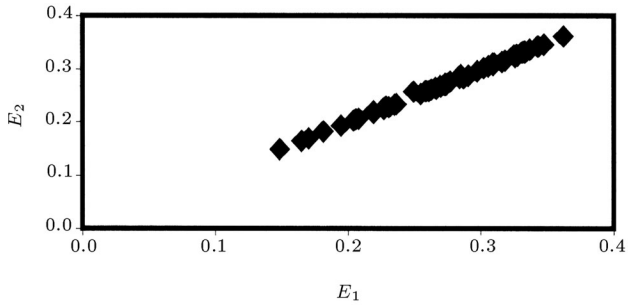

Figure 5. Comparison of specific energy E_1 and E_2 for apex angle = 120°.

30, 60, 90 and 120 degree is 0.59%, 0.55%, 0.72% and 0.94%, respectively. Thus, the assumption of constant energy is accepted for further analysis.

Discharge Coefficient

The discharge coefficient for a sharp crested, triangular side weir may be influenced by: 1) The approach velocity of flow "V_1", 2) Upstream depth of flow "y_1'', 3) Apex angle "θ", 4) Width of main channel "B", 5) Width of side channel "B_1" and 6) Height of weir "w". Dimensional analysis gives:

$$C_m = f\left(F_1, \theta, \frac{B}{B_1}, \frac{w}{y_1}\right), \tag{10}$$

in which $F_1 (= V_1/(gy_1)^{0.5})$ is the upstream Froude number of the flow. Ramamurthy and Carballada [18] showed the effect of B/B_1 on the discharge coefficient. Borghei et al. [15] indicate that this parameter has a secondary effect on C_m. In the present study, B and B_1 were kept constant. Therefore, Equation 10 reduces to:

$$C_m = f\left(F_1, \theta, \frac{w}{y_1}\right). \tag{11}$$

Subramanya and Awasthy [4] and Kumar and Pathak [16] reported that the effect of w/y_1 is insignificant for sharp crested, rectangular and triangular side weirs, respectively. Borghei et al. [15] and Singh et al. [12] believed that the parameter w/y_1 is influencing C_m for a rectangular side weir. However, most of the

investigators have related the discharge coefficient, C_m, to approach Froude number, F_1, only.

The values of C_m were calculated using Equation 8 and measured values of Q_1, y_1, y_2, Q_2, b_1 and w, for all the data. Figures 6 to 9 show the variation of discharge coefficient, C_m, with the most influencing parameter, F_1. The following best-fit equations were obtained for apex angles 30° to 120°, respectively:

$$C_m = 0.6458 - 0.3923F_1 \quad \text{for } \theta = 30°, \tag{12}$$

$$C_m = 0.6108 - 0.3333F_1 \quad \text{for } \theta = 60°, \tag{13}$$

$$C_m = 0.637 - 0.3636F_1 \quad \text{for } \theta = 90°, \tag{14}$$

and:

$$C_m = 0.5973 - 0.1834F_1 \quad \text{for } \theta = 120°. \tag{15}$$

The other influencing parameter is w/y_1. The typical variation of C_m with F_1 for apex angle 120° is shown in Figure 10. The data used in this figure are those with $w/y_1 = 0$ and $w/y_1 = 0.18 - 0.32$. This figure shows that for a particular value of apex angle ($\theta = 120°$), C_m, in addition to F_1 is also, a function of w/y_1. Similar results may be obtained from Figures 11 to 13, which are plots of C_m versus F_1 for various values of w/y_1 and apex angles 90°, 60° and 30°, respectively. Therefore, for a particular value of an apex angle, one can write $C_m = f(F_1, w/y_1)$.

To validate the effect of parameters F_1 and w/y_1 and in accordance with the equations proposed by Singh et al. [12] and Jalili and Borghei [19], C_m for a particular value of an apex angle, can be written as the following linear equation:

$$C_m = a + bF_1 + c\frac{w}{y_1}, \tag{16}$$

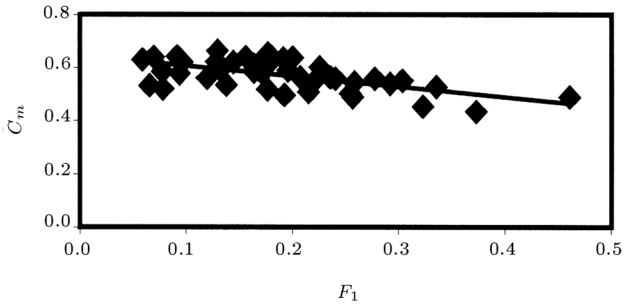

Figure 6. Variation of C_m with F_1 for apex angle = 30°.

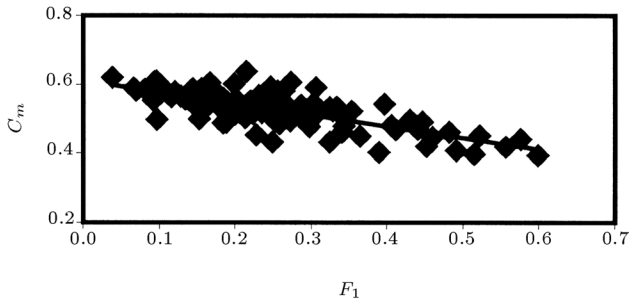

Figure 7. Variation of C_m with F_1 for apex angle = 60°.

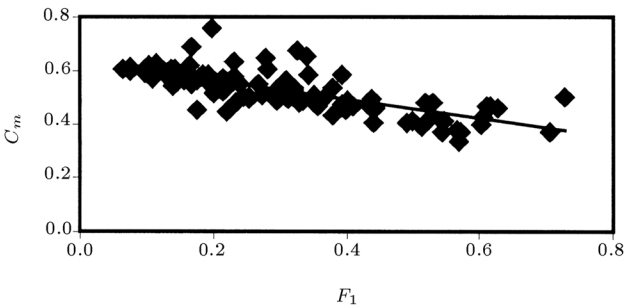

Figure 8. Variation of C_m with F_1 for apex angle = 90°.

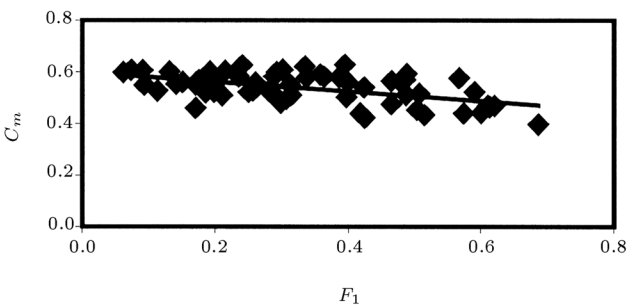

Figure 9. Variation of C_m with F_1 for apex angle = 120°.

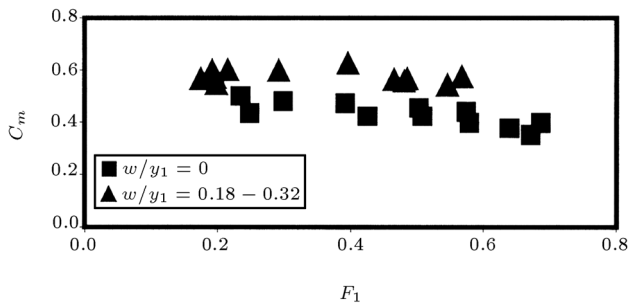

Figure 10. Variation of C_m with F_1 and w/y_1 for apex angle = 120°.

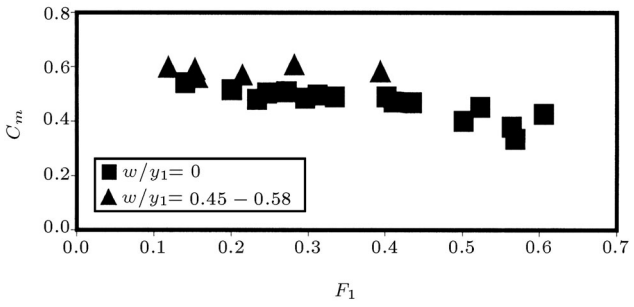

Figure 11. Variation of C_m with F_1 and w/y_1 for apex angle = 90°.

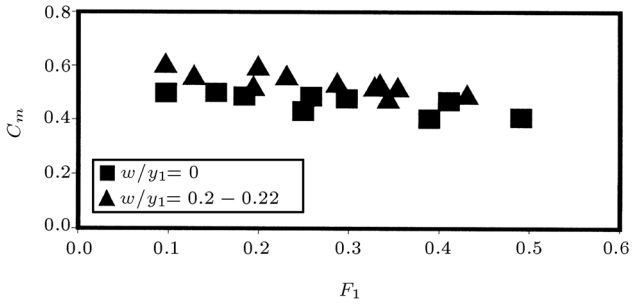

Figure 12. Variation of C_m with F_1 and w/y_1 for apex angle = 60°.

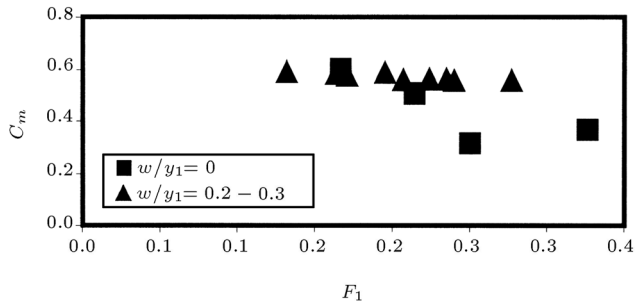

Figure 13. Variation of C_m with F_1 and w/y_1 for apex angle = 30°.

where a, b and c are constants, which can be found using the experimental data. Using the least square method, the following equations were obtained for various values of an apex angle:

$$C_m = 0.6246 - 0.367F_1 + 0.196\frac{w}{y_1} \quad \text{for } \theta = 30°, \tag{17}$$

$$C_m = 0.5707 - 0.2932F_1 + 0.1426\frac{w}{y_1} \quad \text{for } \theta = 60°, \tag{18}$$

$$C_m = 0.5607 - 0.2511F_1 + 0.1661\frac{w}{y_1} \quad \text{for } \theta = 90°, \tag{19}$$

$$C_m = 0.5523 - 0.1317F_1 + 0.0868\frac{w}{y_1} \quad \text{for } \theta = 120°. \tag{20}$$

To have a numerical measure for the best-fit line and its ability, in terms of representing the agreement between observed and computed values of a discharge coefficient, an average percentage error term, ε, was defined as [14,20]:

$$\varepsilon = \frac{100}{N}\sum_{i=1}^{N}\left|\frac{C_{mc} - C_{mo}}{C_{mo}}\right|, \tag{21}$$

in which N is the number of data and C_{mc} and C_{mo} are the computed and observed values of the discharge coefficient, respectively. The computed values of ε for all the obtained equations for C_m are presented in

Table 2. Average percentage error in C_m using different equations.

Equation No.	$C_m = f()$	ε (%)
12	F_1	6.92
13	F_1	5.71
14	F_1	7.05
15	F_1	7.83
17	F_1 and w/y_1	6.02
18	F_1 and w/y_1	4.97
19	F_1 and w/y_1	5.97
20	F_1 and w/y_1	7.18

Table 2. This table shows the comparison of average percentage error, ε, obtained when C_m was related to F_1 (Equations 12 to 15) and when C_m was related to F_1 and $\frac{w}{y_1}$ (Equations 17 to 20). It is obvious that using Equations 17 to 20 improves the average percentage error. Because use of these equations generally leads to lower values of ε (Table 2), Equations 17 to 20 are preferred and can be taken as a discharge coefficient in the DeMarchi equation for subcritical flow.

Equations 4, 8 and 17 to 20 afford a means of calculating the discharge over sharp crested triangular side weirs of apex angles 30° to 120°, respectively.

APPLICATION

Design Procedure

The design of the side weir to pass a certain discharge, Q_s, into the side channel, involves the determination of the side channel width, B_1, and weir height, w, for given values of the upstream discharge, Q_1. For design discharge, B_1 is kept equal to b_1. The steps for design are as follows:

1. For a side weir with known apex angle θ, assume a suitable value for w;
2. Calculate Q_2, using $Q_2 = Q_1 - Q_s$;
3. Calculate normal depth of flow, y_2, and, hence, specific energy, E_2, by:

$$E_2 = y_2 + \frac{Q_2^2}{2gB^2y_2^2}; \tag{22}$$

4. By assuming that specific energy remains constant along the length of the side weir, i.e., $E_1 = E_2 = E$, determine y_1 using the following equation:

$$E_1 = y_1 + \frac{Q_1^2}{2gB^2y_1^2}; \tag{23}$$

5. Calculate F_1 and, hence, C_m from Equations 17 to 20, as the case may be;

6. Determine value of b_1 from Equation 8. If this value is much different from the width of the proposed side channel, B_1, suitable changes may be made in w and the procedure is repeated until $b_1 \cong B_1$.

Discharge Calculation

Computation of the discharge over a given side weir (with known values of θ and w) into a side channel of known width B_1, is possible for given values of y_1 and Q_1. The steps to be followed are as follows:

1. For the depth of flow and discharge in the upstream section, y_1 and Q_1, calculate E_1 using Equation 23;
2. Determine value of F_1 and, hence, C_m from Equations 17-20, as the case may be;
3. By assuming that $E_1 = E_2 = E$, calculate y_2, using Equation 8, for $b_1 = B_1$ (maximum side weir discharge) or measured value of b_1;
4. Calculate downstream discharge, Q_2, from Equation 4;
5. Determine side weir discharge, Q_s, from Equation 9.

CONCLUSION

It was shown that the DeMarchi equation can be used to estimate the discharge over a sharp crested, triangular side weir. It was observed that the specific energy remains constant along the triangular side weir. The DeMarchi coefficient of discharge for a sharp crested triangular side weir in subcritical flow is a function of the approach Froude number in the main channel, the apex angle of the weir and ratio of weir height to upstream depth of flow. New equations for the discharge coefficient were introduced, which enable determination of side weir discharge. The procedures for design and computation of discharge for a triangular side weir were also introduced.

NOMENCLATURE

A	cross sectional area of flow
B	width of main channel
B_1	width of side channel
b_1	distance between sections 1 and 2 along the weir
C_m	DeMarchi coefficient of discharge
E	specific energy
F_1	approach Froude number
g	acceleration due to gravity
Q	discharge in the channel
Q_s	discharge over side weir
S_f	friction slope
S_0	slope of channel bed
T	top width of channel section
V	average velocity in main channel
w	weir height
x	distance along side weir
y	depth of flow
α	kinetic energy correction factor
ε	average percentage error
θ	apex angle
ϕ	DeMarchi varied flow function
suffixes 1 and 2	denotes the upstream and downstream conditions, respectively

REFERENCES

1. Allen, Y.W. "The discharge of water over side weirs in circular pipes", *Proceedings*, Institution of Civil Engineering, London, **6**, pp 270-287 (1957).
2. Colling, V.K. "The discharge capacity of side weirs", *Proceedings*, Institution of Civil Engineering, London, **6**, pp 288-304 (1957).
3. Frazer, W. "The behavior of side weirs in prismatic rectangular channels", *Proceeding*, Institution of Civil Engineering, London, **6**, pp 305-328 (1957).
4. Subramanya, K. and Awasthy, S.C. "Spatially varied flow over side weirs", *J. Hydr. Engrg., ASCE*, **98**(1), pp 1-10 (1972).
5. Smith, K.V.H. "Computer programming for flow over side weir", *J. Hydr. Engrg., ASCE*, **98**(1), pp 1-10 (1973).
6. El-Khashab, A. and Smith, K.V.H. "Experimental investigation of flow over side weirs", *J. Hydr. Engrg., ASCE*, **102**(9), pp 1255-1268 (1976).
7. Ranga Raju, K.G., Prasad, B. and Gupta, S. "Side weirs in rectangular channels", *J. Hydr. Engrg., ASCE*, **105**(5), pp 547-554 (1979).
8. Hager, W.H. "Hydraulics of distribution channel", *Proc. 20th Congress, IAHR*, Moscow, pp 534-541 (1983).
9. Hager, W.H. "Lateral out flow over side weirs", *J. Hydr. Engrg., ASCE*, **113**(4), pp 491-503 (1987).
10. Uyumaz, A. and Smith, R.H. "Design procedure for flow over side weirs", *J. Irrig. and Drain. Engrg., ASCE*, **117**(1), pp 79-90 (1991).
11. Uyumaz, A. "Side weir in triangular channel", *J. Irrig. and Drain. Engrg., ASCE*, **118**(6), pp 965-970 (1992).
12. Singh, R., Manivannana, D. and Satyanarayana, T. "Discharge coefficient of rectangular side weir", *J. Irrig. and Drain. Engrg., ASCE*, **120**(4), pp 814-819 (1994).
13. Swamee, P.K., Pathak, S.K. and Sabzeh Ali, M. "Side weir using elementary discharge coefficient", *J. Irrig. and Drain. Engrg., ASCE*, **120**(4), pp 742-755 (1994).

14. Ghodsian, M. "Elementary discharge coefficient for rectangular side weir", *Proceeding of 4th International Conference on Civil Engineering*, **IV**, pp 36-42 (1997).

15. Borghei, S.M., Jallili and Ghodsian, M., "Discharge coefficient for sharp crested side weir in subcritical flow", *J. Hydr. Engrg., ASCE*, **125**(10), pp 1051-1056 (1999).

16. Kumar, C.P. and Pathak, S.K. "Triangular side weirs", *J. Irrig. and Drain. Engrg., ASCE*, **113**(1), pp 98-105 (1987).

17. Henderson, F.M., *Open Channel Flow*, Macmillan, New York, N.Y., USA (1966).

18. Ramamurthy, A.S. and Carballada, L. "Lateral weir flow model", *J. Irrig. and Drain. Engrg., ASCE*, **106**(1), pp 9-25 (1980).

19. Jalili, M.R. and Borghei, S.M. "Discussion of discharge coefficient of rectangular side weir", *J. Irrig. and Drain. Engrg., ASCE*, **122**(1), pp 132 (1996).

20. Ghodsian, M. "Viscosity and surface tension effects on rectangular weir flow", *Int. Journal of Engineering Science*, **9**(4), pp 111-117 (1998).